International Journal of Biological Macromolecules 235 (2023) 123827

Contents lists available at ScienceDirect

International Journal of Biological Macromolecules

journal homepage: www.elsevier.com/locate/ijbiomac

Studies on anti-colon cancer potential of nanoformulations of curcumin and succinylated curcumin in mannosylated chitosan

Sourour Idoudi [a], Takwa Bedhiafi [a], Fairooz Sahir [b], Yousef Hijji [c], Shahab Uddin [d], Maysaloun Merhi [e], Said Dermime [e], Nashiru Billa [a,*]

[a] Department of Pharmaceutical Sciences, College of Pharmacy, QU Health, Qatar University, Doha, Qatar
[b] Flow Cytometry Core, Translational Research Institute, Academic Health System, Hamad Medical Corporation, Doha, Qatar
[c] Department of Chemistry, Howard University, Washington DC 20069, USA
[d] Translational Research Institute and Dermatology Institute, Academic Health System, Hamad Medical Corporation, Doha, Qatar
[e] Translational Cancer Research Facility, National Center for Cancer Care and Research, Hamad Medical Corporation, Doha, Qatar

ARTICLE INFO

Keywords:
Curcumin
Mannose
Chitosan nanoparticles
Colorectal cancer
Cytotoxicity

ABSTRACT

Colon cancer (CRC) is the second leading cause of death and the third most diagnosed cancer worldwide. Although curcumin (CUR) has demonstrated a potent anticancer activity, it is characterized by its poor solubility, low bioavailability, and instability. This study is a projection from a previous investigation where CUR and succinylated CUR (CUR.SA) were separately encapsulated in mannosylated-chitosan nanoparticles (CM-NPs) to form CUR-NPs and CUR.SA-NPs, respectively. Here, we aim to assess the anti-CRC activity of these two nanoformulations. Cytotoxicity studies using CCK-8 assay indicated that both CUR-NPs and CUR.SA-NPs have a dose and time-dependent toxicity towards CRC human cell-lines (HCT116 and SW480), and more cytotoxic compared to free CUR or CUR-SA in a time-dependent manner. A significant induction of early and late apoptosis in the CUR-NPs and CUR.SA-NPs treated CRC cell lines compared to untreated cells was observed. Western blotting analyses confirmed the induction of apoptosis through activation of Caspase signaling compared to untreated cells. Based on the physicochemical properties of CUR-NPs and CUR.SA-NPs along with the data from the *in vitro* studies, we may conclude these nanoparticle formulations hold very promising attributes, worthy of further investigations for its role in the management of CRC.

1. Introduction

Cancer is one of the most devastating diseases to plague mankind, with increased incidences reported annually [1,2]. Colorectal cancer (CRC) like other cancers along the gastrointestinal tract (GIT), manifests as uncontrolled growth of cells originating from the epithelia of the gastrointestinal tract (GIT) [3]. CRC is the second leading cause of deaths and the third most prevalent cancer type [4]. Current treatment options include radiotherapy, chemotherapy, immunotherapy or surgery [5–7]. These options are either invasive or associated with toxicities, side effects, drug resistance or relapse [8,9]. This calls for concerted efforts by researchers and clinicians to emerge newer treatment strategies that are devoid of the above constraints — a move that will ensure better treatment outcomes. One traction that holds the key to evolving anticancer agents that manifests fewer side effects is in the use of natural anticancer compounds [10–12]. In this regard, curcumin (CUR) has received significant attention in the last decade as a possible anti CRC agent [13–15]. CUR is found in turmeric (*Curcuma longa*), which is a spice native to India [16]. It is the subject of intense interests because of its various biological activities including anti-inflammatory, antibacterial, anti-oxidant, wound healing, and anticancer properties [17–19]. On the other hand, restricted clinical applications of CUR is imposed by its poor solubility in aqueous media, high instability, and rapid metabolism by the liver [20–22]. To derive the full potential of CUR, some form of formulation intervention is necessary or modification to the CUR molecule [23,24]. CUR encapsulated in nanoformulations have been found to present better anti-CRC outcomes compared to pure CUR [25–28]. CUR has also been chemically modified with various moieties in order to effect better solubility [29–31]. The choice of the carrier system that encapsulates CUR also plays a crucial role in determining fate of CUR after deployment at tumor site [32]. Chitosan (CS) is isolated from the shells of crustaceans and has been successfully used to

* Corresponding author at: Pharmaceutical Sciences Department, College of Pharmacy, Qatar University, Qatar.
E-mail address: nbilla@qu.edu.qa (N. Billa).

https://doi.org/10.1016/j.ijbiomac.2023.123827
Received 20 November 2022; Received in revised form 5 February 2023; Accepted 21 February 2023
Available online 27 February 2023

encapsulate CUR in anticancer studies [28,33,34]. In our previous work, we combined chemical modification of CUR with nanoencapsulation to evaluate the anti-CRC effects of CUR [35]. The newly synthesized succinylated curcumin (CUR.SA) presented a better solubility than CUR. The CUR and CUR-SA conjugate were encapsulated in mannosylated-chitosan (CM) nanoparticles *via* ionic gelation, forming CUR-NPs and CUR.SA-NPs, respectively. In the present study, we aim to evaluate the anti-CRC properties of the CUR-NPs and CUR.SA-NPs against CRC cell lines (SW480 and HCT116), through cytotoxicity, morphological, cell cycle and apoptosis using flow cytometry, and protein expression evaluations.

2. Materials and methods

2.1. Materials

Curcumin (mixture of curcumin, desmethoxycurcumin, and bisdemethoxycurcumin) and chitosan (MW: 100–300 kDa) were purchased from Acros Organics. D-Mannose and ethanol (≥99.8 %) were purchased from Honeywell Fluka. Succinic anhydride (≥99 %) and dimethyl sulfoxide (DMSO) (≥99.9 %) were purchased from Sigma Aldrich. Sodium tripolyphosphate (STPP) was purchased from Alfa Aesar. Other organic chemical and solvents used were of reagent grade.

2.2. Formulation of CUR.SA-loaded CM nanoparticles

CUR-NPs and CUR.SA-NPs were prepared as reported previously by Idoudi et al. [35]. Briefly, a 100 μL of STPP (1 mg/mL) solution was added dropwise to a 1 mL CM solution (in 2 % acetic acid) and 1 ml of CUR/CUR.SA (1 mg/ml in ethanol) was further added. The resulting solution was stirred for 30 min, then centrifuged at 4000*g* for 15 min. Finally, the obtained supernatant was transferred to Eppendorf® microcentrifuge tubes and stored for subsequent analyses. Blank mannosylated chitosan nanoparticles (CM-NPs) were similarly prepared.

2.3. Physical characteristics of CUR.SA-NPs and CUR-NPs

The physical characteristics of the nanoparticles was carried as described by Idoudi et al. [35]. In addition, morphological changes of the nanoparticles in cell culture media was assessed in 1× Gibco® DMEM (Thermo Fisher Scientific, USA), and 1× Gibco® RPMI media (Thermo Fisher Scientific, USA). Both media were supplemented with 10 % Gibco® fetal bovine serum (Thermo Fisher Scientific, USA), 1 % PenStrep antibiotic (Thermo Fisher Scientific, USA), and 1 % Gibco® GlutaMAX (Thermo Fisher Scientific, USA) [36]. The morphological change in the incubated nanoparticles at 37 °C and over 48 h in the above medium was assessed using atomic force microscopy (AFM), after placing drops from the media on mica sheets and air-dried. The cantilever was operated at a force constant of 0.7 $N{\cdot}m^{-1}$, frequency of 150 kHz, and over a scan area of 5 × 5 μm.

2.4. In vitro cell evaluation of formulations

2.4.1. Maintenance of cell culture media

Human colorectal adenocarcinoma cell lines (HCT116 and SW480) were cultivated in RPMI and DMEM medium, respectively, supplemented with 10 % FBS and 1 % penicillin-streptomycin. Both cell types were incubated at 37 °C and supplied with 5 % CO_2 until 70–80 % confluence was reached. The state of the cells was assessed daily under optical light microscope at 10× magnification (Nikon Eclipse TS100, Japan).

2.4.2. Cell cytotoxicity

The cytotoxic effects of CUR-NPs and CUR.SA-NPs on SW480, HCT116 CRC cell lines, and non-malignant colon CCD841 CoN cells was assessed using a cell counting Kit-8 (CCK8) assay with WST-8 reagent (Cat. No: 5015944001, Sigma-Aldrich, USA). These cells were used as they express the major mutations in CRC and are among the most aggressive CRC cell lines. Cells were cultured in 96 well plates (Thermo Fisher Scientific, USA) at 5000 cells/well for 24 h, at 37 °C in a CO_2 incubator. The cells were treated with free CUR, CUR.SA conjugate, CUR-NPs and CUR.SA-NPs at 1, 10, and 25 μM of CUR or CUR.SA for 24 and 48 h. Cells in medium alone, DMSO and CM-NPs (50 μM) acted as controls. The cell viability was determined at each time point using a spectrophotometer (Teccan, Switzerland).

2.4.3. Cell cycle analysis

Cellular distribution at the different phases of cell cycle was assessed using flow cytometry after treatment of SW480 and HCT116 cell lines. For this purpose, the cells were seeded in T-75 flasks for 24 h to allow adherence, then they were treated with 10 μM and 25 μM of CUR-NPs and CUR.SA-NPs. Untreated cells served as a control. After treatment for 24 h, the cells were trypsinized and centrifuged at 1300 rpm for 5 min. Further, 1×10^6 cells were collected, centrifuged at 300*g* for 5 min, and re-suspended in 300 μL PBS. 700 μL of 100 % ethanol was added drop by drop while vortex mixing for cell fixation, then the cells were kept at 4 °C overnight. The next day, the cells were washed and centrifuged at 500*g* for 5 min, re-suspended in 250 μL propidium iodide (PI)/RNase staining solution (Cat. No. 550825), incubated at room temperature for 15 min, centrifuged at 500*g* for 5 min, and the cells pellet was re-suspended in 250 μl PBS. Finally, cell cycle analysis was performed using BD LSR Fortessa flow cytometer. The data was analyzed using BD FACS DIVA software.

2.4.4. Cell apoptosis analysis

Cells were seeded in T-75 flasks for 24 h then treated with 10 μM and 25 μM of CUR-NPs and CUR.SA-NPs. Untreated cells were considered as control. After 24 h, cells were trypsinized, and 5×10^5 cells were collected and centrifuged at 1300 rpm for 5 min. The cellular pellet was suspended in 94 μl Annexin Binding Buffer (Cat. No. 556454), 5 μl FITC-Annexin V (Cat. No. 556419) and 1 μL PI (Cat. No. 556463). Further, cells were incubated for 30 min in the dark at 25 °C, washed with 250 μl PBS, and finally analyzed using BD LSR Fortessa flow cytometer. The data was analyzed using BD FACS DIVA software.

2.4.5. Western blotting

For the Western blotting analyses, cells were seeded using T75 flasks and each treated separately with 10 and 25 μM of CUR-NPs and CUR.SA-NPs equivalent to the weights of CUR and CUR.SA, respectively. After incubation for 24 h, 50 μg proteins were collected and quantified using Rapid Gold bicinchoninic acid (BCA) Protein assay kit (Thermo Scientific, USA). Proteins were separated using sodium-dodecyl sulfate polyacrylamide gel electrophoresis, then transferred to polyvinylidene difluoride (PVDF) membrane. Membranes were added to primary antibodies: (i) cleaved poly adenosine diphosphate-ribose polymerase (PARP) (9542S, 1:1000, Cell Signaling Technology, USA); and (ii) cleaved Caspase 8 (9496S, 1:1000, Cell Signaling Technology, USA), and β-actin (1:1000, 4970 L, Cell Signaling Technology, USA) was used as a loading control. The obtained membranes were incubated at 4 °C overnight. Subsequently, the membrane was washed with tris buffer saline-tween (TBST) washing buffer and incubated in horseradish peroxidase-conjugated goat anti-rabbit polyclonal immunoglobulin G secondary antibody (Cat. No. sc-2004, 1:2000, Santa Cruz Biotechnology) for 1 h. The bands were further detected using enhanced chemiluminescence solution (Broaddus) and visualized using a Chem-iDoc™ MP imaging system (BioRad, USA). The densitometric analysis of proteins was performed using image J software.

2.5. Statistical analyses

All presented data are expressed as average of mean ± SD of at least three independent replicates (n = 3). Statistical significance of the data

was determined using a one-way ANOVA and Student's *t*-test, as required, using GraphPad Prism 9 software. The difference was considered statistically significant at *p*-values < 0.05.

3. Results and discussion

3.1. Physical integrity of nanoparticles in culture media

To assess the physical integrity of the CM-NPs, CUR-NPs, and CUR.SA-NPs under typical cell growing conditions, these were incubated in DMEM and RPMI and the changes in morphology over time were assessed using AFM. Fig. 1 shows that there was a slight increase in size of the CUR-NPs and CUR.SA-NPs after 48 h of incubation, as opposed to CM-NPs, which remained largely unchanged. This size increase is expected since proteins in the culture media can react with the nanoparticles and cause charge condensation. This will cause the particles to aggregate as observed in the drug-loaded nanoparticles [37]. We recall that the CM-NPs had a zeta potential of 41.2 mV; whilst CUR-NPs and CUR.SA-NPs had zeta potentials of 11.0 and 13.6 mV respectively [35]. Since the composition of DMEM and RPMI are different, we also expect that the interactions between media and nanoparticles will differ. Nanoparticle aggregation in cell culture media is common, and may compromise on the ability of the particles to be taken-up efficiently by tumor due to size build-up. In this regard, Ozturk et al. proposed that nanoparticles should be decanted after sufficient incubation period and adequate cellular uptake from cell media in order to avoid their aggregation [38].

If the nanoparticles are taken-up rapidly, aggregation will not be a constraint to their deployment in cells. We believe that due to the size of the nanoparticles employed in the present study and the presence of the mannose moieties, the particles would be taken-up sooner than aggregation ensues, however this hypothesis has not been tested.

3.2. In vitro anti-CRC evaluation of nanoformulations

3.2.1. Cell cytotoxicity

Fig. 2 illustrates the viability percentage of SW480 cells in response to treatment with free CUR, CUR.SA conjugate, CM-NPs, CUR-NPs, and CUR.SA-NPs. In Fig. 2A, we observe a decrease in the cell viability with increase in CUR-NPs concentrations during 24 h of exposure. A significant difference in dose response was observed after treatment with CUR-NPs compared to free CUR at 10 and 25 μM ($p < 0.05$). A similar observation was made ($p < 0.05$) with CUR.SA-NPs treatment at 10 and 25 μM compared to free CUR.SA conjugate. Furthermore, there was a significant difference in cell viability at 48 h following treatment with CUR-NPs and CUR.SA-NPs compared to free CUR (Fig. 2B) ($p < 0.05$). Similarly, in HCT116 cell line, (Fig. 3A) a significant decrease in cell viability was observed upon CUR-NPs treatment (10 μM) compared to free CUR ($p < 0.05$) after 24 h, and after CUR.SA-NPs treatment (1 μM) as compared to CUR.SA conjugate ($p < 0.05$). As in HCT116 cells, 48 h treatment (Fig. 3B) with CUR-NPs or CUR.SA-NPs on SW480 induced a higher level of cytotoxicity ($p < 0.05$) compared to free CUR treated cells. Crucially, no cytotoxic effect was observed (Fig. 4) in SW480 and HCT116 cells during 48 h of treatment with free succinic anhydride (SA) (10 and 100 μM), noting that SA was conjugated to CUR for improving its solubility. Thus, CUR and CUR.SA are both more cytotoxic encapsulated in the CM carrier than when administered as free drug. Furthermore, the cytotoxic effect of CUR was retained after conjugation to SA, and potentiated after encapsulation in CM. Equally important is the fact that the blank nanoparticles or CM showed no cytotoxic effects on the cells, as observed by Ma et al. on CRC cells [39]. Both CUR-NPs and CUR.SA-NPs appear to possess identical level of cytotoxicity on SW480 and HCT116 cell lines and significantly higher than free CUR. In concert with the current study, Sorasitthiyanukarn et al. developed CS-alginate nanoparticles containing CUR diethyl disuccinate that showed an enhanced anticancer effect compared to free CUR [28]. According to Fig. 5, treatment of non-malignant CCD841 CoN cells showed no cytotoxic effect over 24 and 48 h of cell treatment, illustrating the safe profile of the prepared CUR-NPs and CUR.SA-NPs against normal cells and their potential application for cancer therapy.

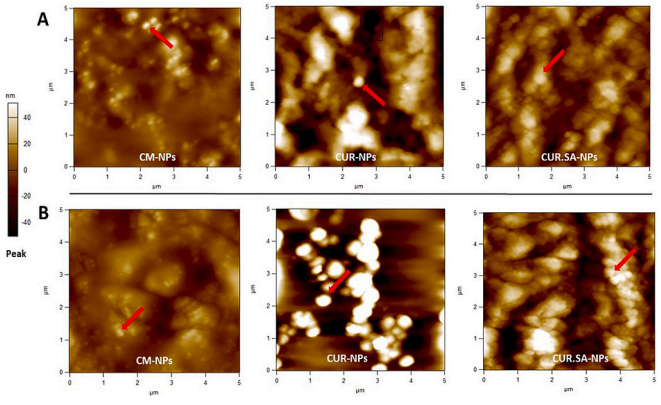

Fig. 1. Change in morphology of nanoparticles after incubation in DMEM: (A) and RPMI: (B) culturing media for 48 h.

The IC_{50} of CUR-NPs and CUR.SA-NPs on SW480 and HCT116 cell lines are displayed in Table 1. Treatment of SW480 and HCT116 with CUR-NPs or CUR.SA-NPs for 48 displayed lower IC_{50} values compared to free CUR and CUR.SA respectively, which illustrates that nanoparticles possess a dose and time-dependent anti-CRC effect on the cells, probably potentiated due to the mucoadhesive properties of the nanoparticles [33]. It could also be a result of the mannose moieties on CM, mannose is reported to attenuate colitis-associated tumorigenesis *via* targeting tumor-associated macrophages (TAM) [40].

3.2.2. Morphology of CRC cell lines after treatment

A phase-contrast inverted microscope was used to observe morphological changes in SW480 and HCT116 cells prior to and after treatment with free CUR, CUR.SA conjugate, CUR-NPs, and CUR.SA-NPs. Prior to treatment, the SW480 cells appeared flattened and attached to the surface of the culture flask (Fig. 6A). Upon treatment with 10 μM of free CUR, CUR.SA, CUR-NPs, and CUR.SA-NPs, the cells became spherical, with cytoplasmic shrinkage. Several cells appear dead and floating in the media with whitened cytoplasm (blue arrows). Cell detachment and departure was observed upon treatment with 25 μM of free CUR, CUR.SA, CUR-NPs, and CUR.SA-NPs. In the case of HCT116 cells, a similar observation was made upon increasing concentrations of treatment (Fig. 6B).

3.2.3. Cell cycle

Cell proliferation at the different cell cycle stages was assessed after treatment of SW480 and HCT116 with CUR-NPs and CUR.SA-NPs (Fig. 7). In the SW480 cell line (Fig. 7A), treatment with 10 μM and 25 μM of CUR-NPs and CUR.SA-NPs caused a significant alteration in the distribution of cells in the different cell cycle phases. A 45.8 ± 10.9 % and 54.1 ± 0.7 % of cell accumulation in G2/M phase was observed after treating cells with 10 μM and 25 μM CUR-NPs respectively, compared to untreated cells (33.2 ± 3.0 %). This was followed by a decrease in cell number in the G0/G1 phase in treated cells (39.4 ± 0.3 % at 10 μM, and 24.6 ± 4.0 % at 25 μM of CUR-NPs) compared to untreated cells. A similar profile was observed with 10 μM and 25 μM CUR.SA-NPs (Fig. 7A) showing cell accumulation in the G2/M phase, followed by a decrease in the G0/G1 phase. Similarly, the HCT116 cell lines (Fig. 7B) exhibited a significantly altered distribution following treatment with 10 μM or 25 μM of CUR-NPs and CUR.SA-NPs, with cell accumulation in the G2/M and a decrease in cell number in the G0/G1 phases. In a recent study, similar outcomes were observed with a cetuximab-conjugated modified citrus pectin-chitosan nanoparticles entrapping CUR, where

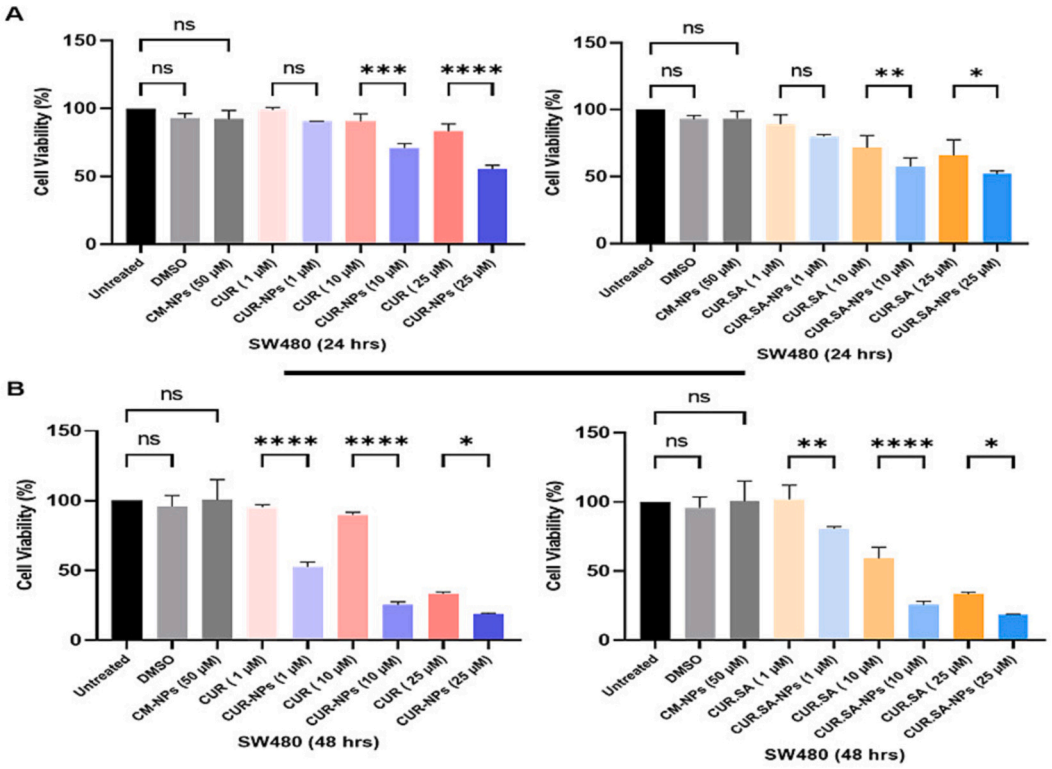

Fig. 2. SW480 cell viability after 24-h treatment using CCK-8 assay: (A) and after 48 h: (B). Data expressed as percentage of untreated cells (control). Cell viability levels <75 % indicative of cytotoxicity. Error bars = SD with n = 3. Statistical significance was calculated using 1-way ANOVA and Šidák test (ns: not significant; *$p < 0.05$, **$p < 0.01$; ***$p < 0.001$, ****$p < 0.0001$ indicates statistical significance).

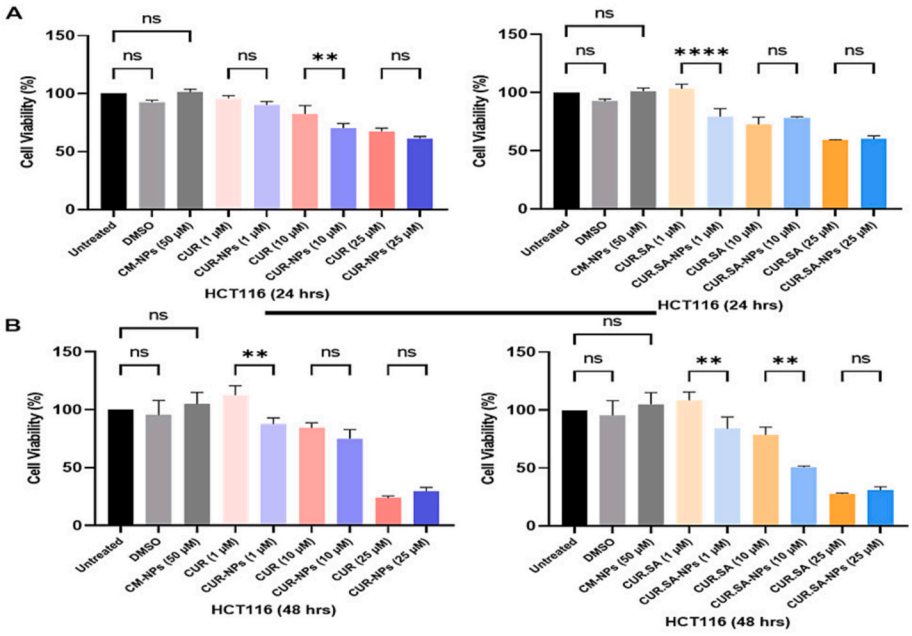

Fig. 3. HCT116 cell viability after 24-h treatment using CCK-8 assay: (A) and after 48 h: (B). Data expressed as percentage of untreated cells (control). Cell viability levels <75 % indicative of cytotoxicity. Error bars = SD with n = 3. Statistical significance was calculated using 1-way ANOVA and Šidák test (ns: not significant; *$p < 0.05$, **$p < 0.01$; ***$p < 0.001$, ****$p < 0.0001$ indicates statistical significance).

the nanoparticles induced Caco-2 cells accumulation in the G2/M phase and cell death [33]. In related study, a 75 μM of a mucoadhesive CUR nanoparticles also induced cell cycle arrest at G2/M phase after a 24-h treatment [41]. It is noteworthy that accumulation of cells in G2/M phase suggests that CUR inhibits cellular proliferation in both SW480 and HCT116 cells, which advances to apoptosis, as discussed below. In the present study, the molecular mechanisms of CUR-SA-NPs -induced G2/M phase arrest in HCT116 and SW480 cells might be associated with upregulation of p21 level and downregulation of the levels of CDK1 and cyclin B as reported by others studies [42]. Moreover, a study by Guo

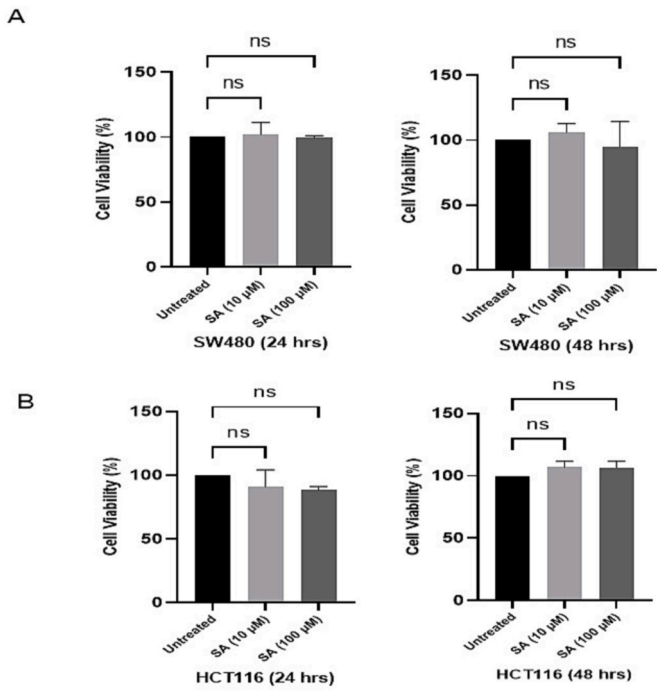

Fig. 4. Cell viability of SW480: (A) and HCT116: (B) treated with free SA (10 and 100 μM), after 24 and 48 h using CCK-8 assay. Data expressed as percentage of untreated (control). Viable cell levels <75 % taken to indicate cytotoxic induction. Error bars = SD with n = 3. Statistical significance calculated using 1-way ANOVA and Dunnett's test (ns: not significant; $*p < 0.05$, $**p < 0.01$; $***p < 0.001$, $****p < 0.0001$ indicate statistical significance).

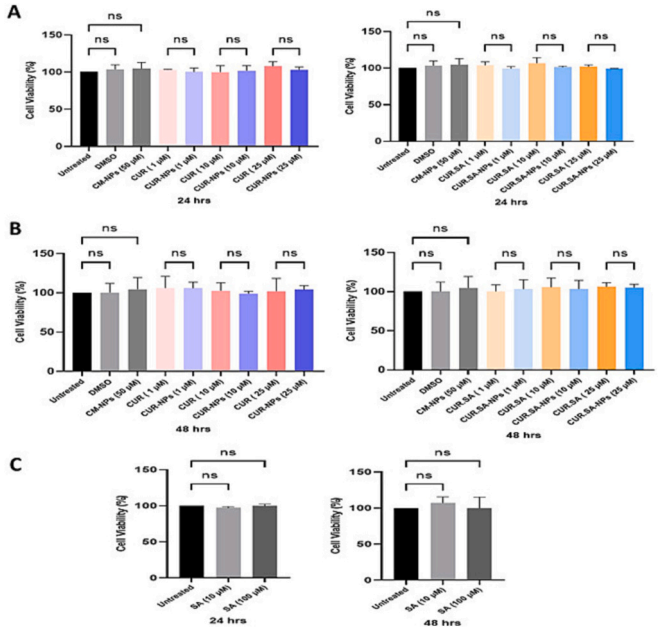

Fig. 5. Cell viability of non-malignant CCD841 CoN cells after 24-h treatment using CCK-8 assay: (A) and after 48 h: (B) using CUR-NPs and CUR.SA-NPs, and with free SA (10 and 100 μM): (C). Data expressed as percentage of untreated cells (control). Cell viability levels <75 % indicative of cytotoxicity. Error bars = SD with n = 3. Statistical significance was calculated using 1-way ANOVA and Šidák test (ns: not significant; $*p < 0.05$, $**p < 0.01$; $***p < 0.001$, $****p < 0.0001$ indicate statistical significance).

Table 1
IC_{50} of CUR-NPs and CUR.SA-NPs on SW480 and HCT116. Each value is a mean of three readings (n = 3).

	24 h		48 h	
	SW480	HCT116	SW480	HCT116
Free CUR (μM)	73.38 ± 3.96	31.01 ± 3.63	21.53 ± 2.77	20.85 ± 3.74
CUR-NPs (μM)	28.75 ± 2.74	31.42 ± 1.44	10.92 ± 3.22	15.92 ± 2.71
Free CUR.SA (μM)	51.28 ± 1.10	28.80 ± 2.12	17.17 ± 0.24	19.50 ± 2.54
CUR.SA-NPs (μM)	27.27 ± 4.56	31.42 ± 1.44	10.81 ± 0.30	17.93 ± 2.92

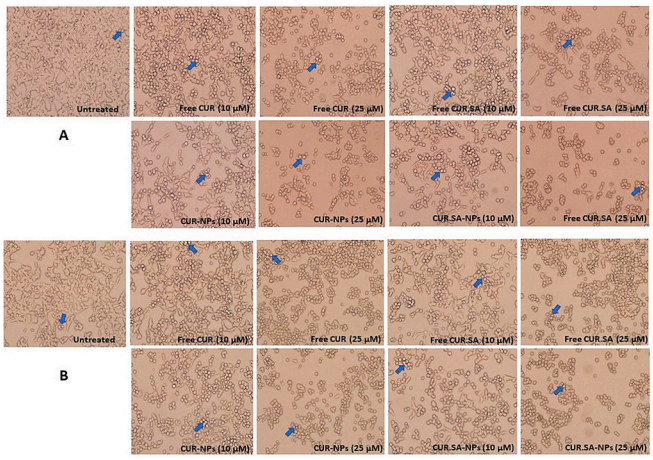

Fig. 6. Representative microscopic images of cells showing morphological changes in SW480 (A) and HCT116 (B) cells after different treatments for 24 h. Morphological features were observed under an inverted microscope with objective lens ×20.

et al. showed that the release of curcumin promotes p53 signaling by increasing p53 expression, which results apoptosis in colon cancer cell lines [43].

3.2.4. *Cell apoptosis*

Investigation on the apoptotic propensity of CUR-NPs and CUR.SA-NPs was determined after treatment with 10 and 25 μM of each on SW480 and HCT cells (Figs. 8 & 9, respectively) using flow cytometry. In SW480 cells (Fig. 8), the population of total apoptotic cells was 5.3 ± 0.2 % for untreated cells, and 8.2 ± 1.7 % for CUR-NPs (10 μM). When the treatment dose was increased to 25 μM of CUR-NPs, total apoptotic cells accounted for 25.4 ± 1.2 % of cell population. A similar dose-response profile was obtained for CUR.SA-NP at 10 μM (8.0 ± 1.2 %) and 25 μM (26.2 ± 1.2 %). In HCT116 cell line (Fig. 9), an increase in total apoptotic cells was also noticed after cell treatment with CUR-NPs (10 and 25 μM) and CUR.SA-NPs (10 and 25 μM), compared to untreated cells. Thus, both CUR-NPs and CUR.SA-NPs appear to stimulate apoptosis of both cell types in a dose-dependent manner ($p < 0.05$), with comparable apoptotic propensities between CUR-NPs and CUR.SA-NPs at 10 and 25 μM. A key point noteworthy is that although CUR.SA is more soluble than CUR [44], we did not observe superior apoptotic effect of CUR.SA in encapsulated nanoparticles on CRC cells. However, an increased accumulation of cells in G2/M phase is indicative of enhanced cytotoxic effect in CRC cells [45], which affirms the *in vitro* cytotoxicity of CUR-NPs and CUR.SA-NPs against SW480 and HCT116 cell lines. Notwithstanding, more studies are needed to ascertain impact of solubility of the drug cargo on apoptosis. It was previously reported by Peihua et al. that CUR induced CRC cancer cell apoptosis [46]. Similarly, Bolat et al. reported that CUR-piperine emulsomes inhibited cell

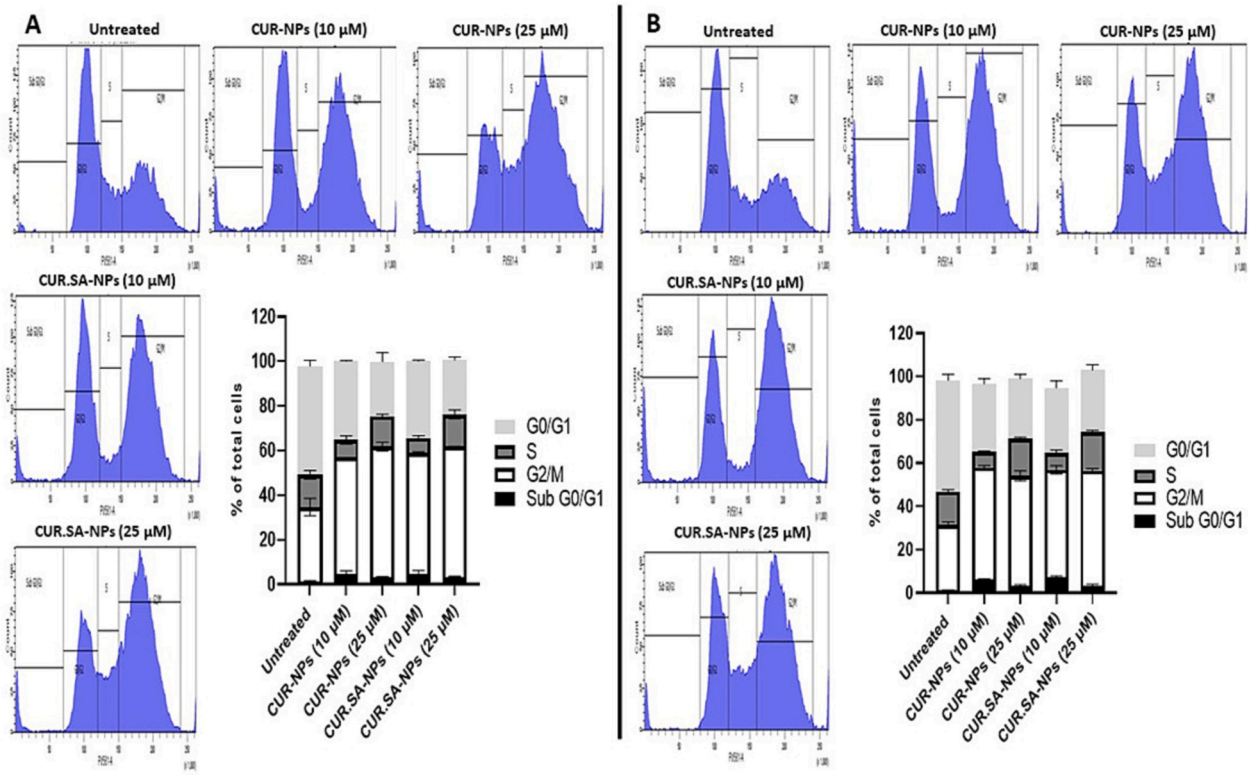

Fig. 7. Cell cycle population in SW480 cells: (A) and HCT116 cells: (B) after treatment with CUR-NPs (10 and 25 μM), CUR.SA-NPs (10 and 25 μM), and untreated cells for 24 h. Characteristic histogram data of Annexin V-FITC/PI flow cytometry evaluation and cell cycle distribution percentages are represented. Results are expressed as percentage of total cells mean ± SD (n = 3).

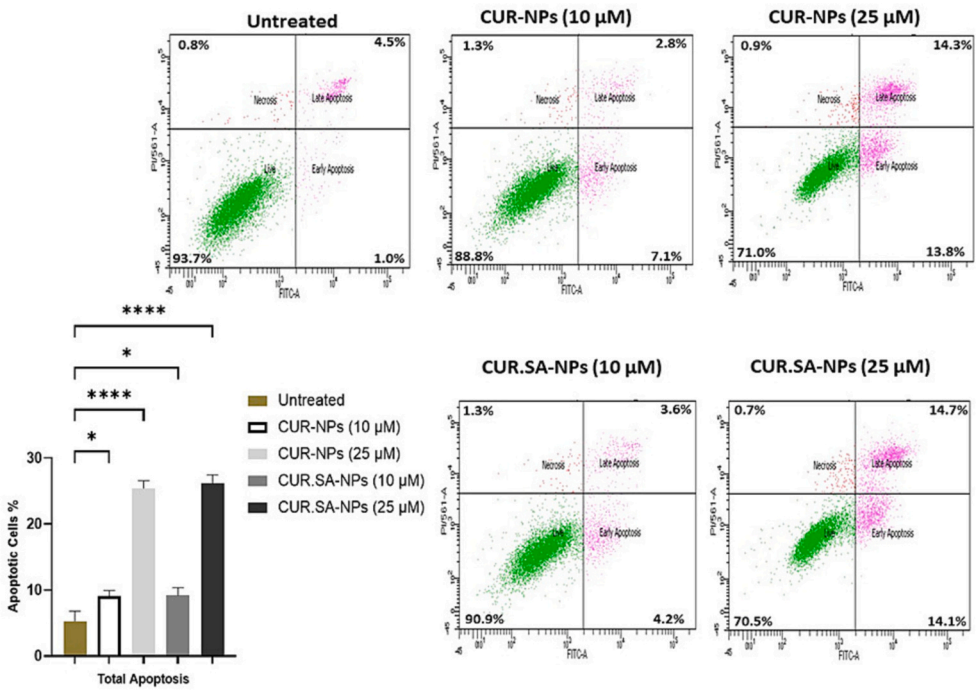

Fig. 8. Total apoptotic cell death of SW480 cells after treatment with CUR-NPs (10 and 25 μM), CUR.SA-NPs (10 and 25 μM), and untreated cells for 24 h. Characteristic histogram data of Annexin V-FITC/PI flow cytometer evaluation, and total apoptotic cell percentages are represented as mean ± SD (n = 3). Statistical significance was calculated using 1-way ANOVA and Dunnett's test (ns: not significant; *$p < 0.05$, **$p < 0.01$; ***$p < 0.001$, ****$p < 0.0001$ indicates statistical significance).

proliferation, and induced apoptosis [47].

3.2.5. Western blotting

To confirm the induction of apoptosis by CUR-NPs and CUR.SA-NPs treatment on SW480 and HCT116 cell lines, the expression of total PARP and Cleaved Caspase 8, which are proapoptotic markers in CRC cells was studied using Western blotting (Fig. 10). In both cell lines (Fig. 11), a significant activation of Caspase 8 and PARP was observed upon treatment of cells with doses of CUR-NPs and CUR.SA-NPs compared to untreated cells ($p < 0.05$), thus confirming apoptosis induction. In a study

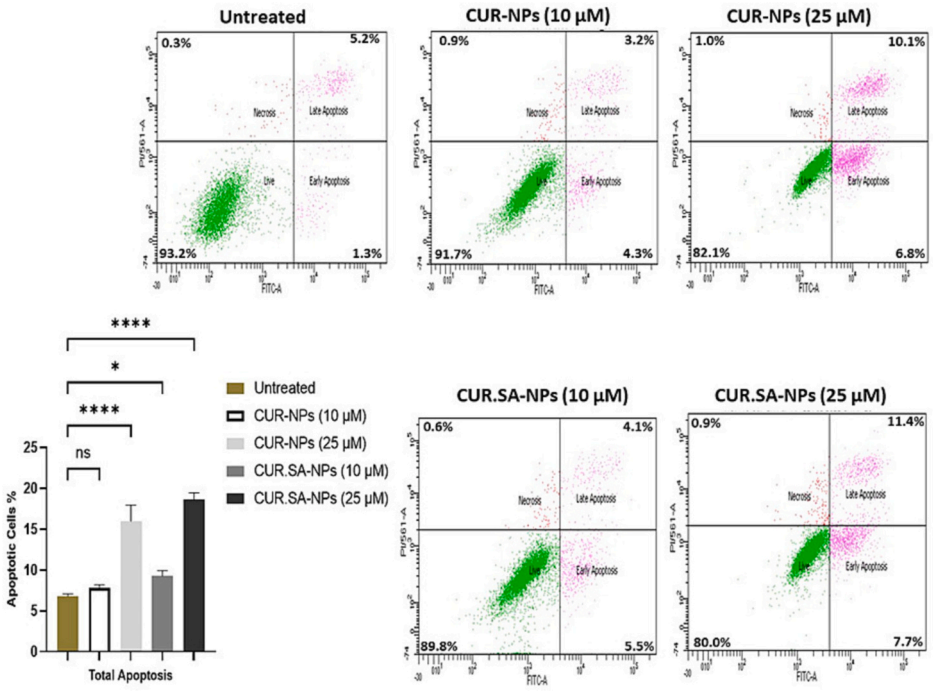

Fig. 9. Total apoptotic cell death of HCT116 cells after treatment with CUR-NPs (10 and 25 μM), CUR.SA-NPs (10 and 25 μM), and untreated cells for 24 h. Characteristic histogram data of Annexin V-FITC/PI flow cytometer evaluation, and total apoptotic cell percentages are represented as mean ± SD (n = 3). Statistical significance was calculated using 1-way ANOVA and Dunnett's test (ns: not significant; *$p < 0.05$, **$p < 0.01$; ***$p < 0.001$, ****$p < 0.0001$ indicates statistical significance).

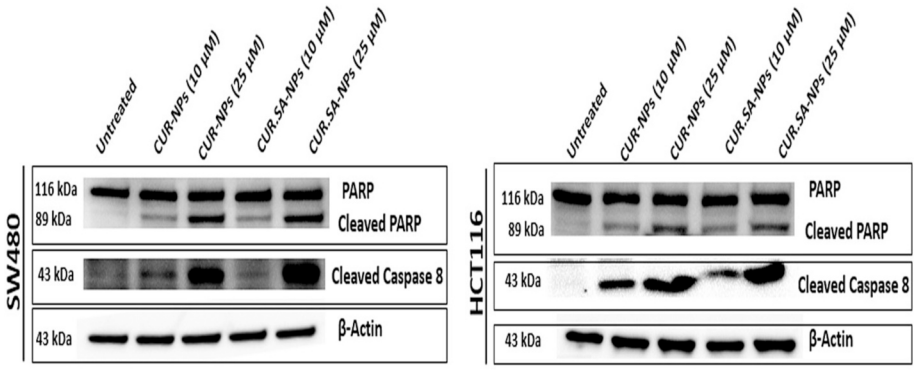

Fig. 10. Western blot bands of total PARP and cleaved Caspase 8 in SW480 and HCT116 cell lines. Increased expression of both total PARP and Cleaved Caspase 8 was noticed after treatment with CUR-NPs and CUR.SA-NPs (10 and 25 μM), and untreated cells for 24 h.

by Shakibaei et al., 20 μM combination of CUR with 5-FU induced apoptosis in HCT116 *via* Caspase 8 and PARP overexpression [48], with identical biological activity as observed in the present work. No statistical difference was observed in the degree of apoptosis or the expression of relevant proteins after treatment with CUR-NPs and CUR.SA-NPs in either cell lines. Initiation of apoptosis requires the Caspase family activation. In the present study, both CUR-NPs and CUR.SA-NPs induced activation of Caspase-8 into Cleaved Caspase-8 (Fig. 10) and the cleavage of the PARP protein into 110 kDa (pro-form) and 89 kDa (cleaved form) fragments due the Caspase-3 activation (Fig. 10). After treatment using both CUR-NPs and CUR.SA-NPs, PARP and the cleaved PARP levels were about 2 times overexpressed compared to the control group ($p < 0.05$; Fig. 11A). Since the formulations yield caspase 8, 3 and PARP fragments, it is possible that the mechanism of apoptosis is a combination of mitochondrial-dependent as well as mitochondrial-independent pathway for the execution of apoptotic cell death.

4. Conclusion

CUR has undoubted anti-cancer properties, but it is poorly soluble and has low bioavailability following oral administration. It is believed that this is the main constraint that limits its effectiveness as a potential antitumor agent. Our research team attempted to develop mannosylated chitosan nanoformulations of CUR and a more soluble version of CUR, which is CUR.SA. When loaded inside mannosylated chitosan nanoparticles, both CUR-NPs and CUR.SA-NPs have presented significant anti-tumor effect against CRC cell lines compared to free CUR, with no significant effect against non-malignant cell lines, illustrating the safe profile of CUR-NPs and CUR.SA-NPs towards normal cells. Clearly, our novel nanoformulations CUR-NPs and CUR.SA-NPs could be a promising strategy to treat other types of cancer.

CRediT authorship contribution statement

Conceptualization: NB; initial draft: SI; data curation: SI, TB, FS; supervision: NB, YMH, MM, SD, SU; reviewing: NB, SI, YMH, MM, SD, SU, TB; statistical analyses: SI, TB; final editing: NB.

Funding

This work was funded by Qatar University Grant No IRCC-2021-006.

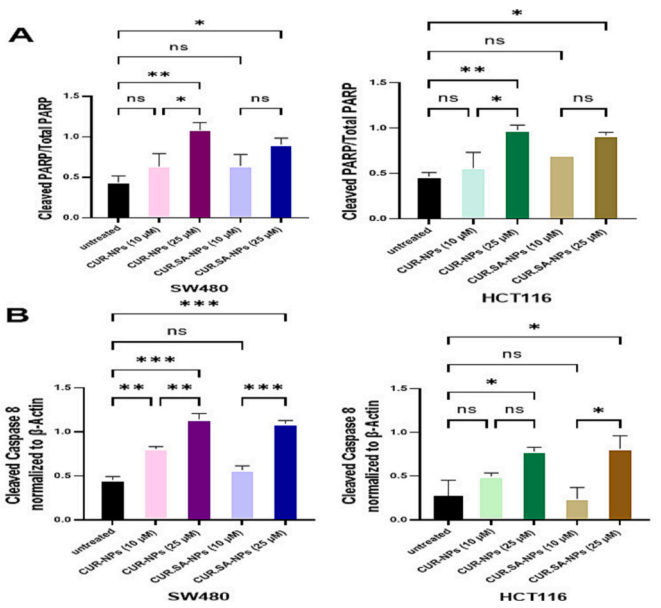

Fig. 11. Quantification of average density of β-actin from cleaved PARP: (A) and Caspase 8: (B). Data expressed as the mean ± SD (n = 2). Statistical significance was calculated using 1-way ANOVA and Bonferroni test (ns: not significant; $*p < 0.05$, $**p < 0.01$; $***p < 0.001$, $****p < 0.0001$ indicates statistical significance).

Declaration of competing interest

The authors declare that they have no known competing financial interests or personal relationships that could have appeared to influence the work reported in this paper.

Data availability

Data will be made available on request.

Acknowledgment

Authors acknowledge the Center of Advanced Materials (CAM), and the Central Laboratories Unit (CLU), Qatar University for support in sample analyses. The authors acknowledge Qatar National Library for open-access publication fee.

References

[1] H. Sung, et al., Global cancer statistics 2020: GLOBOCAN estimates of incidence and mortality worldwide for 36 cancers in 185 countries, CA Cancer J. Clin. 71 (3) (2021) 209–249, https://doi.org/10.3322/caac.21660.
[2] H. Nagai, Y.H. Kim, Cancer prevention from the perspective of global cancer burden patterns, J. Thorac. Dis. 9 (3) (2017) 448–451, https://doi.org/10.21037/jtd.2017.02.75.
[3] Z. Jahanafrooz, J. Mosafer, M. Akbari, M. Hashemzaei, A. Mokhtarzadeh, B. Baradaran, Colon cancer therapy by focusing on colon cancer stem cells and their tumor microenvironment, J. Cell. Physiol. 235 (5) (2020) 4153–4166, https://doi.org/10.1002/jcp.29337.
[4] K.D. Miller, et al., Cancer treatment and survivorship statistics, 2022, CA Cancer J. Clin. (2022) 1–28, https://doi.org/10.3322/caac.21731.
[5] K. Ganesh, et al., Immunotherapy in colorectal cancer: rationale, challenges and potential, Nat. Rev. Gastroenterol. Hepatol. 16 (6) (2019) 361–375, https://doi.org/10.1038/s41575-019-0126-x.
[6] J.F.Y. Xie, Y. Chen, Comprehensive review of targeted therapy for colorectal cancer, Signal Transduct. Target. Ther. 5 (22) (2020), https://doi.org/10.1038/s41392-020-0116-z.
[7] L.A. Manzanares-Guevara, A. Licea-Claverie, I. Oroz-Parra, J. Bernaldez-Sarabia, F. Diaz-Castillo, A.F. Licea-Navarro, Smart nanoformulation based on stimuli-responsive nanogels and curcumin: promising therapy against colon cancer, ACS Omega 5 (16) (2020) 9171–9184, https://doi.org/10.1021/acsomega.9b04390.
[8] L. Ding, S. Ma, H. Lou, L. Sun, M. Ji, Synthesis and biological evaluation of curcumin derivatives with water-soluble groups as potential antitumor agents: an in vitro investigation using tumor cell lines, Molecules 20 (12) (2015) 21501–21514, https://doi.org/10.3390/molecules201219772.
[9] R. Baskaran, T. Madheswaran, P. Sundaramoorthy, H.M. Kim, B.K. Yoo, Entrapment of curcumin into monoolein-based liquid crystalline nanoparticle dispersion for enhancement of stability and anticancer activity, Int. J. Nanomedicine 9 (1) (2014) 3119–3130, https://doi.org/10.2147/IJN.S61823.
[10] T.S. Saranya, V.K. Rajan, R. Biswas, R. Jayakumar, S. Sathianarayanan, Synthesis, characterisation and biomedical applications of curcumin conjugated chitosan microspheres, Int. J. Biol. Macromol. 110 (2018) 227–233, https://doi.org/10.1016/j.ijbiomac.2017.12.044.
[11] A. Prostate, B. Cancers, Curcumin and Its Derivatives as Potential Therapeutic Agents in Prostate, Colon and Breast Cancers, 2019.
[12] H. Luo, et al., Naturally occurring anti-cancer compounds: shining from Chinese herbal medicine, Chin. Med. 14 (1) (2019), https://doi.org/10.1186/s13020-019-0270-9.
[13] S. Idoudi, T. Bedhiafi, Y.M. Hijji, N. Billa, Curcumin and derivatives in nanoformulations with therapeutic potential on colorectal cancer, AAPS PharmSciTech 23 (5) (2022), https://doi.org/10.1208/s12249-022-02268-y.
[14] B.N. Shafei LKIA, M.I. Mohamed Ibrahim, Is curcumin at the threshold of therapeutic effectiveness on patients with colon cancer?-A systematic review, Front. Pharmacol. 2 (12) (2021), https://doi.org/10.3389/fphar.2021.707231.
[15] N.I. Ismail, I. Othman, F. Abas, N.H. Lajis, R. Naidu, Mechanism of Apoptosis Induced by Curcumin in Colorectal Cancer vol. 20, no. 10, 2019, https://doi.org/10.3390/ijms20102454.
[16] A. Karthikeyan, N. Senthil, T. Min, Nanocurcumin: a promising candidate for therapeutic applications, Front. Pharmacol. 11 (2020) 1–24, https://doi.org/10.3389/fphar.2020.00487.
[17] M.S. Valencia, et al., Characterization of curcumin-loaded lecithin-chitosan bioactive nanoparticles, Carbohydr. Polym. Technol. Appl. 2 (2021), 100119, https://doi.org/10.1016/j.carpta.2021.100119.
[18] M. Pooresmaeil, H. Namazi, Facile preparation of pH-sensitive chitosan microspheres for delivery of curcumin; characterization, drug release kinetics and evaluation of anticancer activity, Int. J. Biol. Macromol. 162 (2020) 501–511, https://doi.org/10.1016/j.ijbiomac.2020.06.183.
[19] Y.B. Yu, M.Y. Wu, C. Wang, Z.W. Wang, T.T. Chen, J.K. Yan, Constructing biocompatible carboxylic curdlan-coated zein nanoparticles for curcumin encapsulation, Food Hydrocoll. 108 (2020), https://doi.org/10.1016/j.foodhyd.2020.106028.
[20] K.E. Wong, S.C. Ngai, K.G. Chan, L.H. Lee, B.H. Goh, L.H. Chuah, Curcumin nanoformulations for colorectal cancer: a review, Front. Pharmacol. 10 (2019), https://doi.org/10.3389/fphar.2019.00152.
[21] J. Sharifi-Rad, et al., Turmeric and its major compound curcumin on health: bioactive effects and safety profiles for food, pharmaceutical, biotechnological and medicinal applications, Front. Pharmacol. 11 (2020) 1–23, https://doi.org/10.3389/fphar.2020.01021.
[22] M.D. Cas, R. Ghidoni, Dietary curcumin: correlation between bioavailability and health potential, Nutrients 11 (9) (2019) 1–14, https://doi.org/10.3390/nu11092147.
[23] M.A. Tomeh, R. Hadianamrei, X. Zhao, A review of curcumin and its derivatives as anticancer agents, Int. J. Mol. Sci. 20 (5) (2019), https://doi.org/10.3390/ijms20051033.
[24] P. Yadav, A. Bandyopadhyay, A. Chakraborty, K. Sarkar, Enhancement of anticancer activity and drug delivery of chitosan-curcumin nanoparticle via molecular docking and simulation analysis, Carbohydr. Polym. 182 (August 2017) (2018) 188–198, https://doi.org/10.1016/j.carbpol.2017.10.102.
[25] S.A. Sufi, M. Hoda, S. Pajaniradje, V. Mukherjee, S.M. Coumar, R. Rajagopalan, Enhanced drug retention, sustained release, and anti-cancer potential of curcumin and indole-curcumin analog-loaded polysorbate 80-stabilizied PLGA nanoparticles in colon cancer cell line SW480, Int. J. Pharm. 588 (2020), https://doi.org/10.1016/j.ijpharm.2020.119738.
[26] N.G. Kandile, H.M. Mohamed, A.S. Nasr, Novel hydrazinocurcumin derivative loaded chitosan, ZnO, and Au nanoparticles formulations for drug release and cell cytotoxicity, Int. J. Biol. Macromol. 158 (2020) 1216–1226, https://doi.org/10.1016/j.ijbiomac.2020.05.015.
[27] F. G. Ã, J. Ma, Synergistic effect of the anti-PD-1 antibody with blood stable and reduction sensitive curcumin micelles on colon cancer, Drug Deliv. 28 (1) (2021) 930–942, https://doi.org/10.1080/10717544.2021.1921077.
[28] F.N. Sorasitthiyanukarn, C. Muangnoi, P. Rojsitthisak, P. Rojsitthisak, Chitosan-alginate nanoparticles as effective oral carriers to improve the stability, bioavailability, and cytotoxicity of curcumin diethyl disuccinate, Carbohydr. Polym. 256 (2021), https://doi.org/10.1016/j.carbpol.2020.117426.
[29] S. Yadav, et al., Making of water soluble curcumin to potentiate conventional antimicrobials by inducing apoptosis-like phenomena among drug-resistant bacteria, Sci. Rep. 10 (1) (2020) 1–22, https://doi.org/10.1038/s41598-020-70921-2.
[30] S. Wang, et al., Synthesis of water-soluble curcumin derivatives and their inhibition on lysozyme amyloid fibrillation, Spectrochim. Acta - Part A Mol. Biomol. Spectrosc. 190 (2018) 89–95, https://doi.org/10.1016/j.saa.2017.09.010.
[31] R. Sribalan, et al., Synthesis of a water-soluble pyrazole curcumin derivative. In vitro and in vivo AGE inhibitory activity and its mechanism, ChemistrySelect 2 (3) (2017) 1122–1128, https://doi.org/10.1002/slct.201601740.
[32] P.N. Navya, A. Kaphle, S.P. Srinivas, S.K. Bhargava, V.M. Rotello, H.K. Daima, Current trends and challenges in cancer management and therapy using designer nanomaterials, Nano Converg. 6 (1) (2019), https://doi.org/10.1186/s40580-019-0193-2.

[33] R. Sabra, N. Billa, C.J. Roberts, Cetuximab-conjugated chitosan-pectinate (modified) composite nanoparticles for targeting colon cancer, Int. J. Pharm. 572 (2019), 118775, https://doi.org/10.1016/j.ijpharm.2019.118775.
[34] N. Alizadeh, S. Malakzadeh, Antioxidant, antibacterial and anti-cancer activities of β-and γ-CDs/curcumin loaded in chitosan nanoparticles, Int. J. Biol. Macromol. 147 (2020) 778–791, https://doi.org/10.1016/j.ijbiomac.2020.01.206.
[35] S. Idoudi, et al., A novel approach of encapsulating curcumin and succinylated derivative in mannosylated-chitosan nanoparticles, Carbohydr. Polym. 297 (August) (2022), 120034, https://doi.org/10.1016/j.carbpol.2022.120034.
[36] W. Wichitnithad, U. Nimmannit, S. Wacharasindhu, P. Rojsitthisak, Synthesis, characterization and biological evaluation of succinate prodrugs of curcuminoids for colon cancer treatment, Molecules 16 (2) (2011) 1888–1900, https://doi.org/10.3390/molecules16021888.
[37] S. Jesus, et al., Chitosan nanoparticles: shedding light on immunotoxicity and hemocompatibility, Front. Bioeng. Biotechnol. 8 (February) (2020), https://doi.org/10.3389/fbioe.2020.00100.
[38] K. Ozturk, F.B. Arslan, E. Tavukcuoglu, G. Esendagli, S. Calis, Aggregation of chitosan nanoparticles in cell culture: reasons and resolutions, Int. J. Pharm. 578 (2020), https://doi.org/10.1016/j.ijpharm.2020.119119.
[39] Y. Ma, K.J. Thurecht, A.G.A. Coombes, Development of enteric-coated, biphasic chitosan/HPMC microcapsules for colon-targeted delivery of anticancer drug-loaded nanoparticles, Int. J. Pharm. 607 (2021) 1–9, https://doi.org/10.1016/j.ijpharm.2021.121026.
[40] Q. Liu, X. Li, H. Zhang, H. Li, Mannose attenuates colitis-associated colorectal tumorigenesis by targeting tumor-associated macrophages, J. Cancer Prev. 27 (1) (2022) 31–41, https://doi.org/10.15430/jcp.2022.27.1.31.
[41] L.H. Chuah, C.J. Roberts, N. Billa, S. Abdullah, R. Rosli, Cellular uptake and anticancer effects of mucoadhesive curcumin-containing chitosan nanoparticles, Colloids Surf.B Biointerfaces 116 (2014) 228–236, https://doi.org/10.1016/j.colsurfb.2014.01.007.
[42] L. Harini, et al., An ingenious non-spherical mesoporous silica nanoparticle cargo with curcumin induces mitochondria-mediated apoptosis in breast cancer (MCF-7) cells, Oncotarget 10 (11) (Feb. 2019) 1193–1208, https://doi.org/10.18632/ONCOTARGET.26623.
[43] M. Guo, et al., Surface Decoration of Selenium Nanoparticles With Curcumin Induced HepG2 Cell Apoptosis Through ROS Mediated p53 and AKT Signaling Pathways †, 2017, https://doi.org/10.1039/c7ra08796a.
[44] N.B.S. Idoudi, Y. Hijji, T. Bedhiafi, H. Korashy, S. Uddin, M. Merhi, S. Dermime, A novel approach of encapsulating curcumin and succinylated derivative in mannosylated-chitosan nanoparticles, Carbohydr. Polym. (2022), https://doi.org/10.1016/j.carbpol.2022.120034.
[45] H. Wang, et al., Erianin Induces G2/M-phase Arrest, Apoptosis, and Autophagy via the ROS/JNK Signaling Pathway in Human Osteosarcoma Cells In Vitro and In Vivo, 2016, https://doi.org/10.1038/cddis.2016.138.
[46] P. Li, et al., Curcumin selectively induces colon cancer cell apoptosis and S cell cycle arrest by regulates Rb/E2F/p53 pathway, J. Mol. Struct. 1263 (2022), https://doi.org/10.1016/j.molstruc.2022.133180.
[47] Z.B. Bolat, Z. Islek, B.N. Demir, E.N. Yilmaz, F. Sahin, M.H. Ucisik, Curcumin- and piperine-loaded emulsomes as combinational treatment approach enhance the anticancer activity of curcumin on HCT116 colorectal cancer model, Front. Bioeng. Biotechnol. 8 (2020) 1–21, https://doi.org/10.3389/fbioe.2020.00050.
[48] M. Shakibaei, A. Mobasheri, C. Lueders, F. Busch, P. Shayan, A. Goel, in: Curcumin Enhances the Effect of Chemotherapy against Colorectal Cancer Cells by Inhibition of NF- k B and Src Protein Kinase Signaling Pathways vol. 8, no. 2, 2013, pp. 1–13, https://doi.org/10.1371/journal.pone.0057218.